CDSRR has been shown to be caused by mutations in the potassium channel, subfamily V, member 2 (*KCNV2*) gene (MIM# 607,604), which encodes a voltage-gated potassium channel subunit, Kv8.2 [18]. This silent subunit is expressed in rod and cone photoreceptors [18-20], and is thought to assemble with other K^+ channel subunits such as KCNB1, KCNC1, and KCNF1. These subunits form functional heteromeric channels with altered properties that have a narrowed membrane potential for activation and slow inactivation kinetics [19]. Eventually, these kinetic properties result in transient hyperpolarization overshoots on rapid changes in the inward currents [19]. A deficiency of Kv8.2 by a mutation in *KCNV2* may affect the characteristics of the I_{ks} as first described in amphibian photoreceptors [21]. This deficiency may influence the photoreceptor membrane potential. However, the underlying mechanisms that fully explain the clinical features of CDSRR are still not determined.

More than 50 different disease-causing variants in *KCNV2* have been reported: small insertion and deletion changes or large deletions that constitute a protein truncation and single nucleotide changes with amino acid substitutions [9,10,13,14,16,18,22,23]. Three small case series describe the clinical features of CDSRR in East Asians [3,5,15]; however, molecular genetic studies of these populations have not been published. Thus, the purpose of this study was to determine the molecular genetic characteristics from the clinical and electrophysiological findings of four Japanese patients who were diagnosed with CDSRR.

METHODS

Subjects: Four subjects who were diagnosed with CDSRR from the clinical and electrophysiological findings were ascertained at the National Institute of Sensory Organs, National Tokyo Medical Center, Tokyo, Japan and Niigata University, Niigata, Japan. The natural history of these four patients has been partially reported recently [24]. The procedures used were approved by the ethics committee of each institution, and all procedures were performed in accordance with the principles of the Declaration of Helsinki. Informed consent was obtained from all experimental subjects for all procedures.

Clinical assessment: A complete medical history was obtained, and a comprehensive ophthalmological examination was performed on all patients. The photophobia and night blindness episode was obtained on direct questioning. The clinical assessments included measurements of the best-corrected visual acuity (BCVA), dilated ophthalmoscopy, color fundus photography, AF imaging, OCT, and electrophysiological recordings. AF images were obtained with the HRA 2 confocal scanning laser ophthalmoscope (Heidelberg Engineering, Heidelberg, Germany; excitation light, 488 nm; barrier filter, 500 nm; field of view, 30×30°) [25]. The OCT images were obtained with SD-OCT (Cirrus HD-OCT, versions 4.5 and 5.1; Carl Zeiss Meditec, Dublin, CA) [26].

Electrophysiological assessments: Full-field ERGs were recorded from the four patients with the minimum standard protocol of the International Society for Clinical Electrophysiology of Vision (ISCEV) [27]. The ERG examination included the following: (i) dark adapted dim flash 0.01 $cd \cdot s \cdot m^{-2}$ (DA 0.01), (ii) dark adapted bright flash 30.0 $cd \cdot s \cdot m^{-2}$ (DA 30.0), (iii) light adapted 3.0 $cd \cdot s \cdot m^{-2}$ at 2 Hz (LA 3.0), and (iv) light adapted 3.0 $cd \cdot s \cdot m^{-2}$ 30 Hz flicker ERG (LA 3.0 30Hz). The extended protocol included the recording of the dark-adapted ERGs elicited by stimulus intensities of 0.001 $cd \cdot s \cdot m^{-2}$, 0.01 $cd \cdot s \cdot m^{-2}$, 0.3 $cd \cdot s \cdot m^{-2}$, 3.0 $cd \cdot s \cdot m^{-2}$, and 30.0 $cd \cdot s \cdot m^{-2}$. Two of the four patients were also recorded with the extended protocol. An excessive or disproportionate increase in the dark adapted b-wave with increasing flash intensity was assessed in these two patients, according to the previous report [9].

Mutational screening: After informed consent was obtained, blood samples were collected in EDTA tubes from each subject, and the DNA was extracted with a DNA extraction kit (QIAamp DNA Blood Maxi Kit; Qiagen, Venlo, the Netherlands). All exons and exon–intron boundaries were amplified with polymerase chain reaction (PCR), and the primer sequences used are shown in Table 1. PCR was performed with 20 µl volume containing 0.5 Unit Taq polymerase (PrimeStar GXL DNA polymerase, Takara, Tokyo, Japan). The sequence was determined based on the dideoxy terminator method using an ABI PRISM 3100×l Genetic Analyzer (Applied Biosystems, Foster City, CA) according to the manufacturer's protocol. The SeqScape Software version 2.5 (Applied Biosystems) was used to analyze the sequence alignment. Bidirectional Sanger sequencing was also performed in other family members of the proband, to confirm the segregation of the alleles.

Molecular genetic analyses: All of the missense variants identified were analyzed using two software prediction programs, Sorting Intolerant from Tolerance (SIFT) and PolyPhen2 [28,29]. The predicted effects on splicing of all missense variants were assessed with the Human Splicing finder program version 2.4.1. The allele frequency of each variant was estimated with the Exome Variant Server (NHLBI Exome Sequencing Project, Seattle, WA). A multiple sequence alignment program for DNA or proteins, the Clustal Omega, was applied to confirm an evolutionary conservation. Likely non-disease-causing variants (polymorphisms)

Table 1. Primer Sequences and Conditions for *KCNV2* Mutational Screening.

Primer	Sequence (5'–3')	Product size (bp)	PCR annealing (°C)
E1aF	AGGACCTGAGAAGGGGCAGCT	831	71
E1aR	TCCAGGAGGCGGAGGAACTCT		
E1bF	CCCTGCTGTCCACGCTGAATG	799	71
E1bR	CAGCGTGGGTAAGGTGGGTCA		
E1cF	AAGATCCAGCACGAGCTGCGC	841	65
E1cR	ATGGATGTCAAAAGTGGTGGA		
E2aF	AGCTTCTGTTCTTTTCATGAC	624	63
E2aR	GTCTCATAGTTGCTCTGTGTT		

bp = base pairs.

were also analyzed with the same protocol applied to likely disease-causing variants.

RESULTS

The demographic features of the four individuals from three families with CDSRR are summarized in Table 2. There were two siblings (patients 1 and 2) in one family and one case in each of the two families (patients 3 and 4). The pedigree of each family is shown in Figure 1, and a consanguineous marriage was present in family 3.

Clinical findings: The age of the patient at the time of the examination was 23, 17, 21, and 17 years with the age of disease onset at 9, 5, 3, and 2 years (Table 2). Three patients complained of photophobia (patients 1, 2, and 4), and all four patients had night blindness. Patient 4 had had mild nystagmus since age 2 years. The decimal BCVA of the four patients ranged from 0.08 to 0.8, and the BCVA of patients 1 and 2 was better than 0.7 in each eye.

The findings obtained from the color fundus photographs, AF images, and SD-OCT images are summarized in Figure 1 and Table 2. The fundus photographs showed mottling of the RPE at the macula in all four patients with subtle patchy granular flecks at the macula in patient 3. A ring enhancement of the AF signal was detected in the AF images of all four patients; three subjects had it centered on the fovea (patients 1, 2, and 3), and one had it at the parafovea (patient 4). In patient 3, the ring enhancement at the fovea was surrounded by patchy granular foci of the high AF signal at the macula.

SD-OCT demonstrated abnormalities in the outer retinal layers in all four patients. The cone outer segment tip line was absent in the macular area in all patients. The photoreceptor inner and outer segment junction line was discontinuous at the fovea in patients 3 and 4, and thinning of the outer retina was detected at the fovea in all four patients.

Electrophysiological assessments: The electrophysiological findings are summarized in Table 3, and the ERGs are shown in Figure 2. The full-field ERGs were recorded with the minimum ISCEV standard from patients 2 and 3, and extended protocol full-field ERGs including the dark-adapted ERGs elicited by an intensity series were obtained from patients 1 and 4.

The dark adapted b-wave amplitude elicited by a stimulus intensity 0.01 (DA0.01) was delayed and decreased in patients 3 and 4, but was normal but delayed in patient 1. The responses for DA0.01 were undetectable in patient 2. An excessive increase in the b-wave for the extended protocol was found in two patients, 1 and 4. In addition, the a-wave was square-shaped with a supernormal b-wave elicited by stimulus intensity 30.0 (DA 30.0) in all four patients. The photopic ERGs (LA 3.0 and LA 3.0 30Hz) were decreased in all four patients (Table 3 and Figure 2).

Molecular genetics: The molecular genetic findings are summarized in Table 2 and Appendix 1. Likely disease-causing variants in *KCNV2* were identified in all four patients. The four likely disease-causing variants were p.Arg27His, p.Cys177Arg, p.Arg206Pro, and p.Gly461Arg (Appendix 1), and two likely non-disease-causing variants (polymorphisms) were p.Gly61Gly and p.Ala265Ala (Appendix 2). The segregation of each allele was confirmed by screening of other family members for all these variants.

Detailed molecular results including in silico analysis to assist in predicting the pathogenicity of the four disease-causing variants identified are shown in Appendix 1. All of the four likely disease-causing variants were single nucleotide changes with one amino acid substitution (missense), i.e., p.Arg27His, p.Cys177Arg, p.Arg206Pro, and p.Gly461Arg. Compound heterozygosity for the two alleles, p.Cys177Arg and p.Gly461Arg, in patients 1, 2, and 3 and homozygosity for the complex alleles, p.Arg27His and p.Arg206Pro, in patient

Table 2. Summary of demographics, clinical findings and molecular status for four Japanese patients with *KCNV2*-retinopathy

Pt, FM, gender	Onset of disease, age at examination (years)	VA		Fundus		AF		OCT		Mutation status
		RE	LE	RPE mottling	Subtle patchy granular flecks	Ring enhancement	Patchy granular foci of high signal	Absence of COST	Deficit of IS/OS	
1, 1, F	9, 23	0.7	0.8	Macula	ND	Fovea	ND	Fovea	ND	Compund heterozygous [c.529 T>C, p.Cys177Arg]; [c.1381G>A, p.Gly461Arg]
2, 1, M	5,17	0.7	0.7	Macula	ND	Fovea	ND	Fovea	ND	Compund heterozygous [c.529 T>C, p.Cys177Arg]; [c.1381G>A, p.Gly461Arg]
3, 2, F	3,21	0.1	0.1	Macula	Macula	Fovea	Macuala	Macula	Fovea	Compund heterozygous [c.529 T>C, p.Cys177Arg]; [c.1381G>A, p.Gly461Arg]
4, 3, F	2, 17	0.1	0.08	Macula	ND	Para-fovea	ND	Macula	Fovea	Complex homozygous [c.80 G>A, p.Arg27His]; [c.617 G>C, p.Arg206Pro]

Pt = Patient; FM = family number; VA = logMAR visual acuity; RE = right eye; LE = left eye; RPE = retinal pigment epithelium; AF = autofluorescence; COST = cone outer segment tip line; IS/OS = photoreceptor inner and outer segment junction; ND = not detected. The affected area of each finding is based on the color fundus photographs, AF images, and the OCT images in each column.

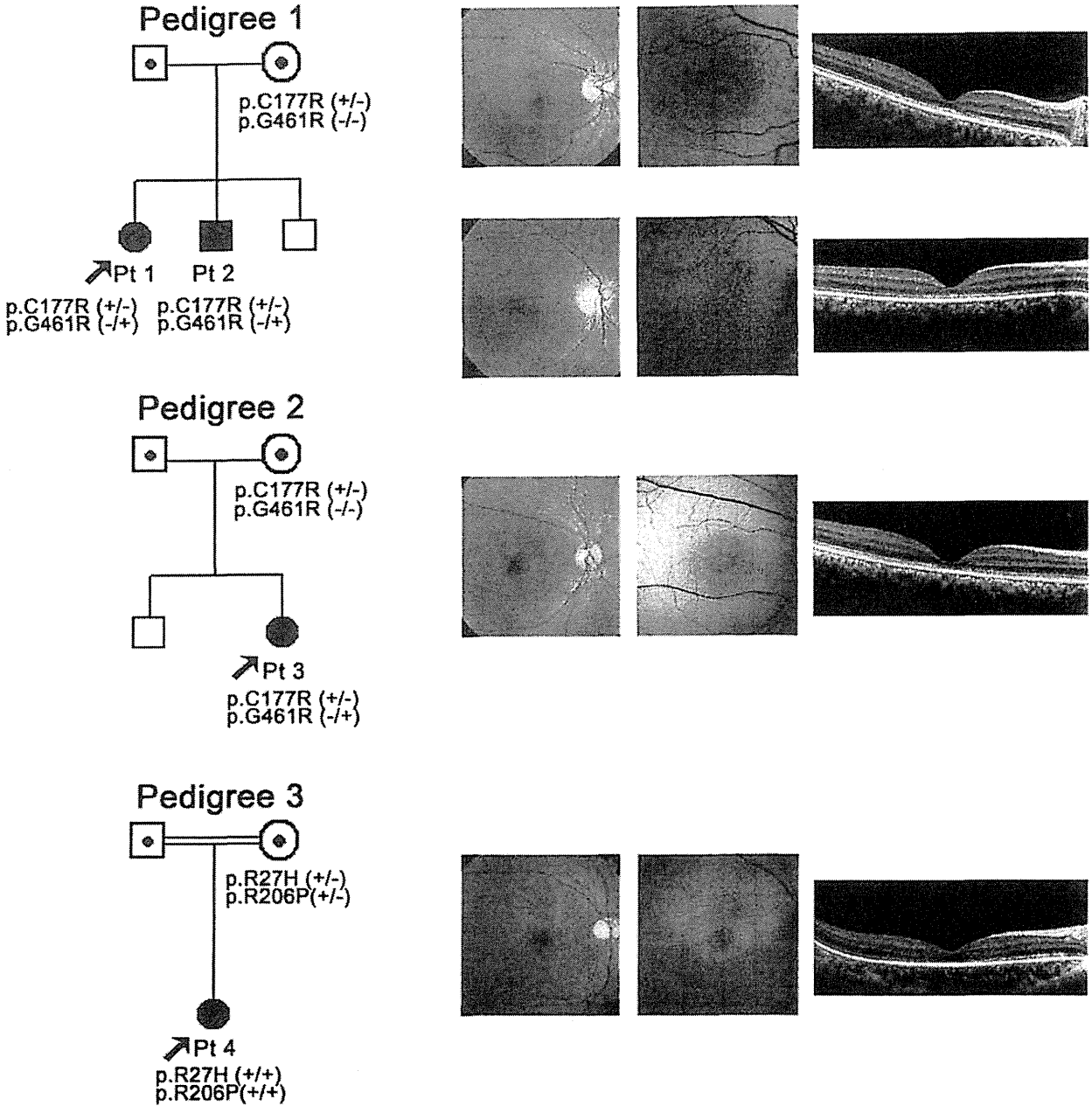

Figure 1. Pedigree and retinal imaging of each patient with potassium channel, subfamily V, member 2 retinopathy. Pedigrees with molecular status of the three families with potassium channel, subfamily V, member 2 (*KCNV2*) retinopathy are shown on the left. Retinal images including color fundus photographs, autofluorescence images, and spectral domain optical coherence tomography are presented on the right. Images of patient 1 (top row), patient 2 (second row from top), patient 3 (third row from top), and patient 4 (bottom row) are shown.

4 were revealed by the segregation analyses. The p.Gly461Arg variant has been reported, and the p.Arg27His, p.Cys177Arg, and p.Arg206Pro variants are putative novel. In silico analysis revealed an "intolerant" protein function or a "probably or possibly damaged" protein but no effect on splicing in the three putative novel variants (SIFT, Poplyphen2, and Human Splicing finder; Appendix 1). The reported missense variant, p.Gly461Arg, with possibly affecting splicing was detected in six out of 13,006 individuals of the Exome Variant Server; the three novel variants, p.Arg27His, p.Cys177Arg, and

Table 3. Electrophysiological Findings of Four Japanese Patients with KCNV2-retionpathy

Pt	DA 0.01		DA 30.0				Square shaped a-wave	Excessive enlargement of b-wave in the extended protocol	LA 3.0			LA 3.0 30Hz		
			A-wave		B-wave				A-wave	B-wave		B-wave		
	Amp (μv)	PT (ms)	Amp	PT	Amp	PT			Amp	PT	Amp	PT	Amp	PT
1	N	Del	N	Del	Super N	NA	(+)	(+)	Sub N	Del	Sub N	UD	UD	UD
2	UD	UD	N	Del	Super N	NA	(+)	NA	Sub N	Del	Sub N	Del	Sub N	Del
3	Sub N	Del	N	Del	Super N	N	(+)	NA	Sub N	Del	Sub N	Del	Sub N	N
4	Sub N	Del	N	Del	Super N	NA	(+)	(+)	Sub N	Del	Sub N	Del	Sub N	Del

Pt = patient; Amp = amplitude; PT = peak time; N = normal; UD = undetectable response; Sub N = subnormal; Del = delayed response; Super N=supernormal response; NA = not available. Full-field electroretinography (ERG) incorporating the standards of the International Society for Clinical Electrophysiology of Vision (ISCEV) included: (i) dark adapted dim flash 0.01 cd•s•m^{-2} (DA0.01), (ii) dark adapted bright flash 30.0 cd•s•m^{-2} (DA30.0), (iii) light adapted 3.0 cd•s•m^{-2} at 2 Hz (LA 3.0), and (iv) light adapted 3.0 cd•s•m^{-2} 30 Hz flicker (LA 3.0 30 Hz). The extended protocol also included the recording of dark adapted responses to an intensity series of flashes in order to detect an excessive enlargement of dark adapted b-wave (patients 1 and 4).

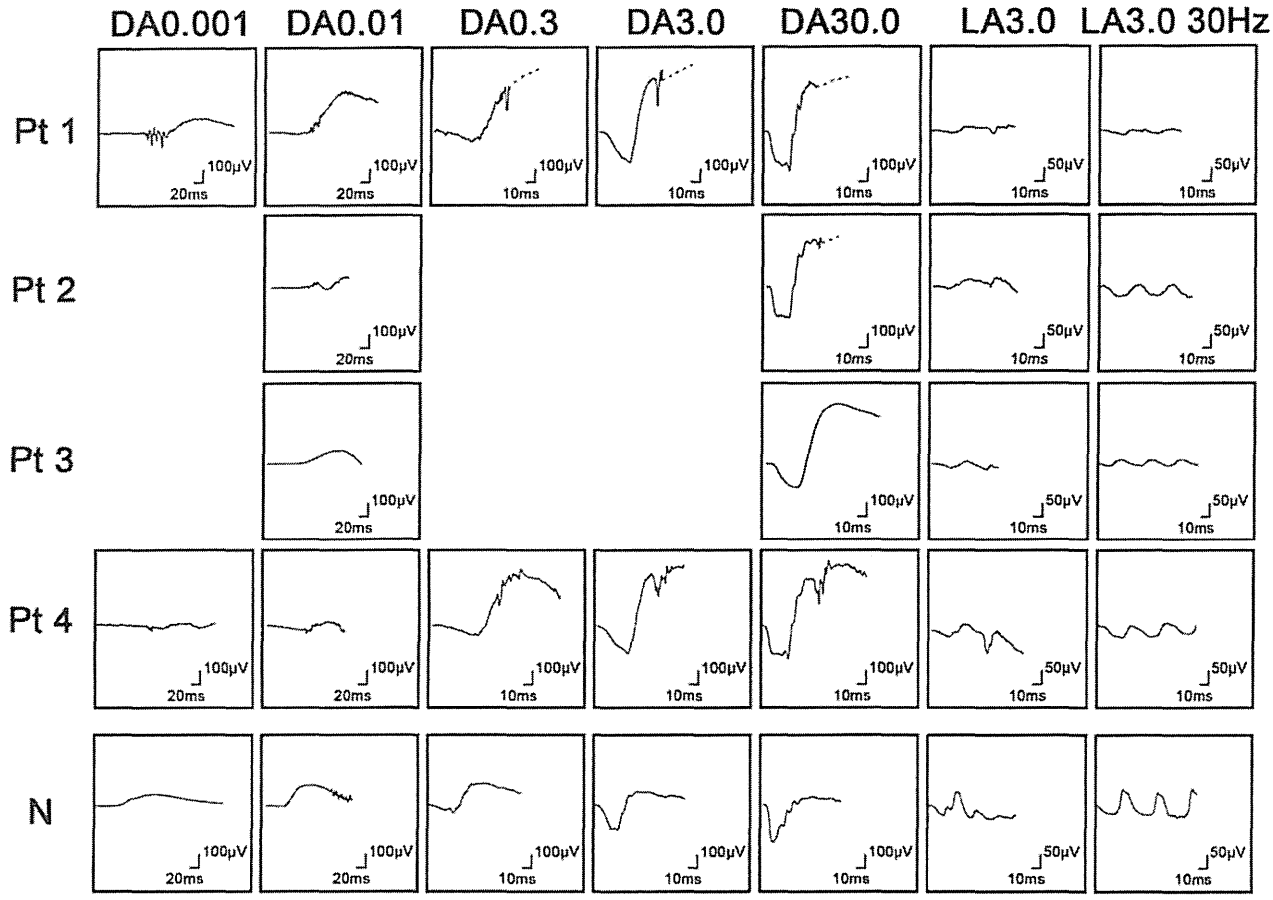

Figure 2. Electrophysiological findings of each patient with potassium channel, subfamily V, member 2 (*KCNV2*) retinopathy. Full-field electroretinograms (ERGs) of patient 1 (top row), patient 2 (second row), patient 3 (third row), and patient 4 (forth row) are shown. The ERGs from a normal control (bottom row) are also shown for comparison. All four patients underwent full-field ERG testing with the minimum standards of the International Society for Clinical Electrophysiology of Vision (ISCEV): (i) dark adapted dim flash 0.01 cd•s•m^{-2} (DA 0.01), (ii) dark adapted bright flash 30.0 cd•s•m^{-2} (DA 30.0), (iii) light adapted 3.0 cd•s•m^{-2} at 2 Hz (LA 3.0), and (iv) light adapted 3.0 cd•s•m^{-2} 30 Hz flicker ERG (LA 3.0 30Hz). The extended protocol was applied to two subjects (patients 1 and 4), including the recording of dark-adapted ERGs to an intensity series of flashes; 0.001 cd•s•m^{-2}, 0.01 cd•s•m^{-2}, 0.3 cd•s•m^{-2}, 3.0 cd•s•m^{-2}, and 30.0 cd•s•m^{-2}.

p.Arg206Pro, were not identified. Three missense variants, p.Arg27His, p.Cys177Arg, and p.Arg206Pro, were highly conserved among the orthologs, and one missense variant, p.Gly461Arg, was completely conserved (Figure 3).

A model of the *KCNV2* protein structure showing the approximate position of the missense disease-causing variants identified is presented in Figure 4. The KCNV2 protein comprises 545 amino acids and contains an N-terminal A and B box (NAB) and six transmembrane domains, (S1–S6), with a K selective motif, GlyTyrGly, in the pore-forming loop (P loop) between S5 and S6 [18]. One variant is located within the N-terminus (p.Arg27His), two variants, p.Cys177Arg and p.Arg206Pro, within the NAB, and one variant, p.Gly461Arg, within the P-loop.

Detailed molecular results of two non-disease-causing variants (polymorphisms) including the in silico analyses are summarized in Appendix 2. These two homozygous variants, p.Gly61Gly and p.Ala265Ala, were synonymous changes in the cording region and were predicted to be benign or have no effect on splicing (Polyphen2 and Human Splicing finder program analysis). Both were present in a high number of chromosomes in the Exome Variant Server database (7647/13006 for p.Gly61Gly and 5636/13006 for p.Ala265Ala, respectively).

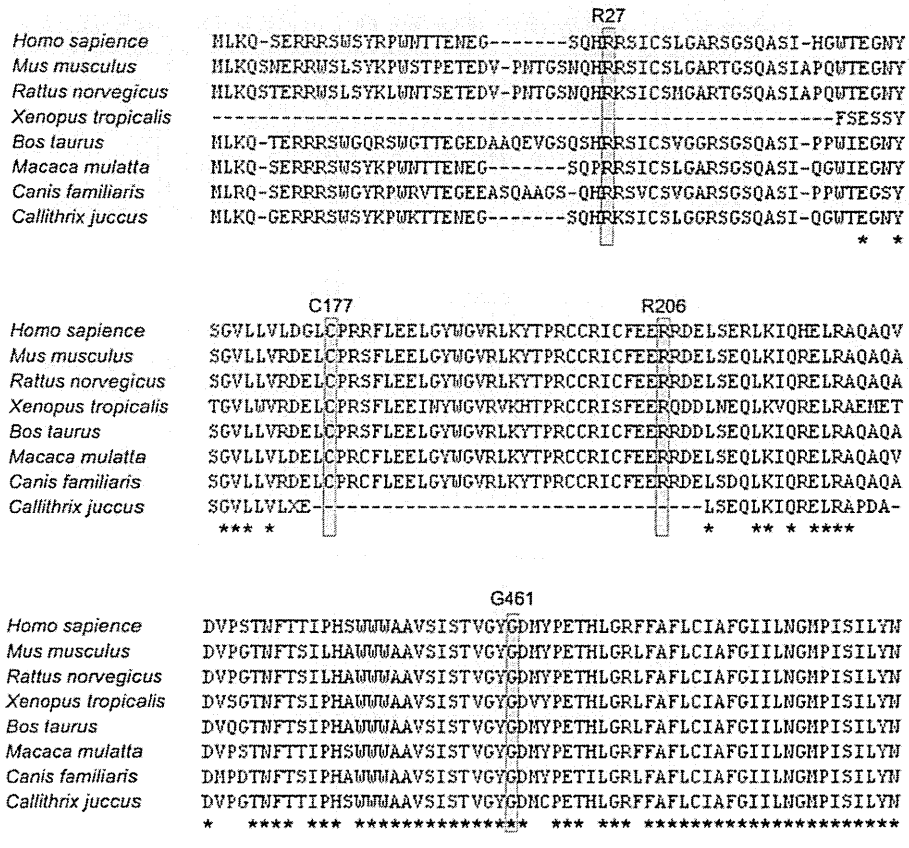

Figure 3. Multiple alignment of eight species of potassium channel, subfamily V, member 2 orthologs. The amino acid-sequence alignment is numbered in accordance with the *Homo sapiens* potassium channel, subfamily V, member 2 (*KCNV2*) sequence (ENSP00000371514). The positions of mutated residues, Arg27 (c.80 G>A, p.Arg27His), Arg177 (c.529 T>C, p.Cys177Arg), Arg206 (c.617 G>C, p.Arg206Pro), and Gly461 (c.1381 G>A, p.Gly461Arg), are highlighted. The alignment was performed with the Clustal Omega program, and the asterisk indicates a completely conserved residue.

DISCUSSION

Our results showed the molecular genetic characteristics of four Japanese patients with CDSRR, which, to the best of our knowledge, is the first report of these characteristics of *KCNV2* retinopathy in an East Asian population. Our four patients harbored the likely disease-causing variants in *KCNV2*. Compound heterozygosity for two alleles, p.Cys177Arg and p.Gly461Arg, in three patients and homozygosity for two complex alleles, p.Arg27His and p.Arg206Pro, in one subject were confirmed. Three of the four variants, p.Arg27His, p.Cys177Arg, and p.Arg206Pro, were novel, which indicates all genotypes identified in our series have never been described before.

The clinical and electrophysiological characteristics of our four patients were similar to those of reported patients [8-11,13,14,17,18]. Additionally, all four patients presented with a decrease in central vision whose onset was in the first decade of life with minimal fundus changes and a characteristic ring enhancement of the AF signal (Table 2 and Figure 1). These findings are also in accordance with earlier reports [9-12,14]. SD-OCT demonstrated a discontinuous or absent inner and outer segment junction line in two patients

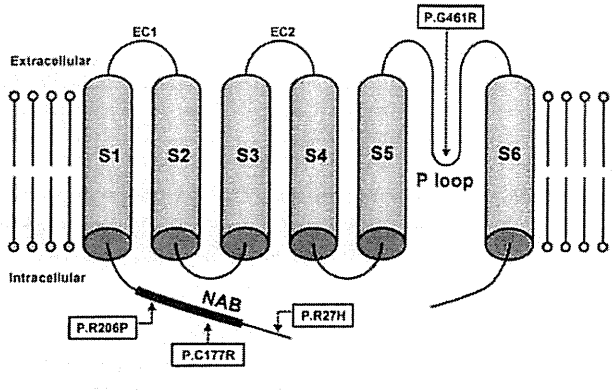

Figure 4. Model of the potassium channel, subfamily V, member 2 protein structure. A schematic representation of the potassium channel, subfamily V, member 2 (*KCNV2*) subunit of the K channel is drawn showing the approximate position of missense disease-causing variants identified in this study. The *KCNV2* protein consists of an N-terminus, an N-terminal A and B box (NAB), and six transmembrane domains (S1–S6), with two extracellular loops (EC 1, 2) and a K selective motif, GlyTyrGly, in the pore-forming loop (P loop) between S5 and S6.

as previously reported [10]. In addition, the absence of the cone outer segment tip line at the macular region was also confirmed in all four patients.

The pathognomonic electrophysiological features were demonstrated in all four patients, viz., delayed and reduced photopic ERGs, delayed ERGs for DA 0.01, and a square-shaped a-wave with a supernormal b-wave for DA 30.0 (Table 3 and Figure 2). An excessive increase in the b-wave for the DA ERGs to an intensity series of flashes was also confirmed in patients 2 and 3. Therefore, the unique rod system abnormalities were identical to those reported for *KCNV2* retinopathy [9,14].

Compound heterozygosity for two alleles, p.Cys177Arg and p.Gly461Arg, was found in patients 1, 2, and 3. The p.Gly461Arg with relatively higher allele frequency affects the third residue of the ultraconserved-GYG-tripeptide motif that acts as an ion selectivity filter in the K channel's pore-forming loop, P loop, between S5 and S6 (Figure 4) [30]. The clinical effect of p.Gly461Arg was well characterized earlier [10,16,17]. Friedburg et al. reported that three siblings with homozygous p.Gly461Arg had a relatively severe phenotype with an early onset and nystagmus at <5 years of age, visual acuity decrease (0.1–0.25, constantly), minimal fundus changes, ring enhancement at the foveal AF image, and an excessive increase in the b-wave for scotopic ERGs to an intensity series [17]. In contrast to the previous reports on homozygous patients, the three patients with heterozygous p.Gly461Arg in our series did not have nystagmus, and two of our patients had less severe BCVA decrease (0.7–0.8). These findings imply that the phenotype of the compound heterozygous for p.Gly461Arg and p Cys177Arg could have a less severe phenotype than those homozygous for p.Gly461Arg. It is of interest that the phenotypic spectrum, compound heterozygous for p.Gly461Arg and p Cys177Arg, was also observed in our series. Two relatively mild phenotypes were observed in the two siblings in our series (patients 1 and 2). In addition, one relatively severe phenotype, with more severe visual acuity decrease (0.1) and photoreceptor/RPE abnormalities at the macula, was detected in patient 3.

Three of the new disease-causing missense variants were located within the N-terminal region of the protein (Figure 4): p.Arg27His within the N-terminus and p.Cys177Arg and p.Arg206Pro within NAB. p.Cys177Arg was completely segregated, and the predicted pathogenesis and evolutionary conservation were confirmed. The coexistence of two likely disease-causing variants, p.Arg27His and p.Arg206Pro, on the same chromosome was also identified in our series with segregation analyses. The patient who was homozygous for these two complex variants had a severe phenotype, with an early onset (2 years), nystagmus, and severe visual acuity decrease (0.1 to 0.08). Both variants were predicted to be pathogenic with evolutionary high conservation (Appendix 1and Figure 3). Whether one of these variants is a neutral polymorphisms in cis with disease-causing one, or whether family 4's alleles are complex with two independently damaging missense variants remains to be determined.

To conclude, this study further delineates the molecular genetic findings of *KCNV2* retinopathy. Three putative novel variants were identified in our four Japanese patients with CDSRR, and our findings suggest there may be a distinct spectrum of *KCNV2* alleles in the Japanese population. However, the clinical findings were similar to that of the reported other population. Electrophysiology was fundamental to the diagnosis with pathognomonic findings due to channelopathy. The pathognomonic characteristics may be a useful method of determining the success of clinical therapeutic trials with gene replacement or pharmacological treatments for channelopathy.

APPENDIX 1. RESULTS OF IN SILICO MOLECULAR GENETIC ANALYSIS OF *KCNV2* MUTATIONS IDENTIFIED.

To access the data, click or select the words "Appendix 1." Pt = patient; Hom = homozygous; Het = heterozygous; SIFT = sorting Intolerant from Tolerance; HSF = human splicing finder program; CV = consensus values; EVS = exome variant server; POD = possibly damaging; PRD = probably damaging; ND = not detected. SIFT (version 4.0.4) results are reported to be tolerant if tolerance index ≥ 0.05 or intolerant if tolerance index < 0.05. Polyphen-2 (vision 2.1) appraises mutations qualitatively as Benign, Possibly Damaging or Probably Damaging based on the model's false positive rate. The cDNA is numbered according to Ensemble transcript ID ENST00000382082, in which +1 is the A of the translation start codon. Human splicing finder version 2.4.1 was applied to predict the effect of each variant on splicing. The results from HSF matrix indicate the values for the wild type and mutant sequences. The larger difference of values between the wild type and the mutant sequences indicates the greater change that the variant can affect on the splice site. EVS denotes variants in the Exome Variant Server, NHLBI Exome Sequencing Project, Seattle, WA.

APPENDIX 2. MOLECULAR ANALYSIS OF *KCNV2* POLYMORPHISMS.

To access the data, click or select the words "Appendix 2." Pt = patient; Hom = homozygous; Het = heterozygous; SIFT = sorting Intolerant from Tolerance; HSF = human splicing

finder program; CV = consensus values; EVS = exome variant server.

ACKNOWLEDGMENTS

We are grateful to the patients who kindly agreed to take part in this study and colleagues who referred individuals to us at National Institute of Sensory Organs. We thank Professor Duco I. Hamasaki (Bascom Palmer Eye Institute, Miami, FL) for proofreading. This research is supported in part by research grants from the Ministry of Health, Labor and Welfare, Japan and Grant-in-Aid for Scientific Research from JSPS.

REFERENCES

1. Gouras P, Eggers HM, MacKay CJ. Cone dystrophy, nyctalopia, and supernormal rod responses. A new retinal degeneration. Arch Ophthalmol 1983; 101:718-24. [PMID: 6601944].
2. Alexander KR, Fishman GA. Supernormal scotopic ERG in cone dystrophy. Br J Ophthalmol 1984; 68:69-78. [PMID: 6607068].
3. Yagasaki K, Miyake Y, Litao RE, Ichikawa K. Two cases of retinal degeneration with an unusual form of electroretinogram. Doc Ophthalmol 1986; 63:73-82. [PMID: 3015524].
4. Foerster MH, Kellner U, Wessing A. Cone dystrophy and supernormal dark-adapted b-waves in the electroretinogram. Graefes Arch Clin Exp Ophthalmol 1990; 228:116-9. [PMID: 2186970].
5. Kato M, Kobayashi R, Watanabe I. Cone dysfunction and supernormal scotopic electroretinogram with a high-intensity stimulus. A report of three cases. Doc Ophthalmol 1993; 84:71-81. [PMID: 8223112].
6. Rosenberg T, Simonsen SE. Retinal cone dysfunction of supernormal rod ERG type. Five new cases. Acta Ophthalmol (Copenh) 1993; 71:246-55. [PMID: 8333273].
7. Hood DC, Cideciyan AV, Halevy DA, Jacobson SG. Sites of disease action in a retinal dystrophy with supernormal and delayed rod electroretinogram b-waves. Vision Res 1996; 36:889-901. [PMID: 8736222].
8. Michaelides M, Holder GE, Webster AR, Hunt DM, Bird AC, Fitzke FW, Mollon JD, Moore AT. A detailed phenotypic study of "cone dystrophy with supernormal rod ERG". Br J Ophthalmol 2005; 89:332-9. [PMID: 15722315].
9. Robson AG, Webster AR, Michaelides M, Downes SM, Cowing JA, Hunt DM, Moore AT, Holder GE. "Cone Dystrophy with Supernormal Rod Electroretinogram": A Comprehensive Genotype/Phenotype Study Including Fundus Autofluorescence and Extensive Electrophysiology. Retina 2010; 30:51-62. [PMID: 19952985].
10. Sergouniotis PI, Holder GE, Robson AG, Michaelides M, Webster AR, Moore AT. High-resolution optical coherence tomography imaging in KCNV2 retinopathy. Br J Ophthalmol 2012; 96:213-7. [PMID: 21558291].
11. Vincent A, Robson AG, Holder GE. PATHOGNOMONIC (DIAGNOSTIC) ERGs A Review and Update. Retina 2013; 33:5-12. [PMID: 23263253].
12. Khan AO, Alrashed M, Alkuraya FS. 'Cone dystrophy with supranormal rod response' in children. Br J Ophthalmol 2012; 96:422-6. [PMID: 21900228].
13. Zobor D, Kohl S, Wissinger B, Zrenner E, Jagle H. Rod and Cone Function in Patients with KCNV2 Retinopathy. PLoS ONE 2012; 7:e46762-[PMID: 23077521].
14. Vincent A, Wright T, Garcia-Sanchez Y, Kisilak M, Campbell M, Westall C, Heon E. Phenotypic Characteristics including in vivo Cone Photoreceptor Mosaic in KCNV2-Related 'Cone Dystrophy with Supernormal Rod Electroretinogram'. Invest Ophthalmol Vis Sci 2013; 30:898-908. .
15. Tanimoto N, Usui T, Ichibe M, Takagi M, Hasegawa S, Abe H. PIII and derived PII analysis in a patient with retinal dysfunction with supernormal scotopic ERG. Doc Ophthalmol 2005; 110:219-26. [PMID: 16328930].
16. Wissinger B, Dangel S, Jagle H, Hansen L, Baumann B, Rudolph G, Wolf C, Bonin M, Koeppen K, Ladewig T, Kohl S, Zrenner E, Rosenberg T. Cone dystrophy with supernormal rod response is strictly associated with mutations in KCNV2. Invest Ophthalmol Vis Sci 2008; 49:751-7. [PMID: 18235024].
17. Friedburg C, Wissinger B, Schambeck M, Bonin M, Kohl S, Lorenz B. Long-term follow-up of the human phenotype in three siblings with cone dystrophy associated with a homozygous p.G461R mutation of KCNV2. Invest Ophthalmol Vis Sci 2011; 52:8621-9. [PMID: 21911584].
18. Wu H, Cowing JA, Michaelides M, Wilkie SE, Jeffery G, Jenkins SA, Mester V, Bird AC, Robson AG, Holder GE, Moore AT, Hunt DM, Webster AR. Mutations in the gene KCNV2 encoding a voltage-gated potassium channel subunit cause "cone dystrophy with supernormal rod electroretinogram" in humans. Am J Hum Genet 2006; 79:574-9. [PMID: 16909397].
19. Czirják G, Toth ZE, Enyedi P. Characterization of the heteromeric potassium channel formed by kv2.1 and the retinal subunit kv8.2 in Xenopus oocytes. J Neurophysiol 2007; 98:1213-22. [PMID: 17652418].
20. Hölter P, Kunst S, Wolloscheck T, Kelleher DK, Stieht C, Wolfrum U, Spessert R. The retinal clock drives the expression of Kcnv2, a channel essential for visual function and cone survival. Invest Ophthalmol Vis Sci 2012; 53:6947-54. [PMID: 22969075].
21. Beech DJ, Barnes S. Characterization of a voltage-gated K+ channel that accelerates the rod response to dim light. Neuron 1989; 3:573-81. [PMID: 2642011].
22. Thiagalingam S, McGee TL, Weleber RG, Sandberg MA, Trzupek KM, Berson EL, Dryja TP. Novel mutations in the KCNV2 gene in patients with cone dystrophy and a supernormal rod electroretinogram. Ophthalmic Genet 2007; 28:135-42. [PMID: 17896311].

23. Wissinger B, Schaich S, Baumann B, Bonin M, Jagle H, Friedburg C, Varsanyi B, Hoyng CB, Dollfus H, Heckenlively JR, Rosenberg T, Rudolph G, Kellner U, Salati R, Plomp A, De Baere E, Andrassi-Darida M, Sauer A, Wolf C, Zobor D, Bernd A, Leroy BP, Enyedi P, Cremers FP, Lorenz B, Zrenner E, Kohl S. Large deletions of the KCNV2 gene are common in patients with cone dystrophy with supernormal rod response. Hum Mutat 2011; 32:1398-406. [PMID: 21882291].

24. Nakamura N, Tsunoda K, Fujinami K, Shinoda K, Tomita K, Hatase T, Usui T, Akahori M, Iwata T, Miyake Y. Long-term Observation over Ten Years of Four Cases of Cone Dystrophy with Super-normal Rod Electroretinogram . Nippon Ganka Gakkai Zasshi 2013; In press.

25. Fujinami K, Tsunoda K, Hanazono G, Shinoda K, Ohde H, Miyake Y. Fundus autofluorescence in autosomal dominant occult macular dystrophy. Arch Ophthalmol 2011; 129:597-602. [PMID: 21555613].

26. Tsunoda K, Usui T, Hatase T, Yamai S, Fujinami K, Hanazono G, Shinoda K, Ohde H, Akahori M, Iwata T, Miyake Y. Clinical characteristics of occult macular dystrophy in family with mutation of Rp111 gene. Retina 2012; 32:1135-47. [PMID: 22466457].

27. Marmor MF, Fulton AB, Holder GE, Miyake Y, Brigell M, Bach M. ISCEV Standard for full-field clinical electroretinography (2008 update). Doc Ophthalmol 2009; 118:69-77. [PMID: 19030905].

28. Ng PC, Henikoff S. SIFT: Predicting amino acid changes that affect protein function. Nucleic Acids Res 2003; 31:3812-4. [PMID: 12824425].

29. Adzhubei IA, Schmidt S, Peshkin L, Ramensky VE, Gerasimova A, Bork P, Kondrashov AS, Sunyaev SR. A method and server for predicting damaging missense mutations. Nat Methods 2010; 7:248-9. [PMID: 20354512].

30. Heginbotham L, Lu Z, Abramson T, MacKinnon R. Mutations in the K+ channel signature sequence. Biophys J 1994; 66:1061-7. [PMID: 8038378].

Articles are provided courtesy of Emory University and the Zhongshan Ophthalmic Center, Sun Yat-sen University, P.R. China. The print version of this article was created on 20 July 2013. This reflects all typographical corrections and errata to the article through that date. Details of any changes may be found in the online version of the article.

Clinical Ophthalmology

Dovepress

CASE REPORT

Two siblings with late-onset cone–rod dystrophy and no visible macular degeneration

Hiroyuki Sakuramoto[1]
Kazuki Kuniyoshi[1]
Kazushige Tsunoda[2]
Masakazu Akahori[2]
Takeshi Iwata[2]
Yoshikazu Shimomura[1]

[1]Department of Ophthalmology, Kinki University Faculty of Medicine, Osaka-Sayama City, Osaka, Japan; [2]National Institute of Sensory Organs, National Hospital Organization Tokyo Medical Center, Tokyo, Japan

Background: We report our findings in two siblings with late-onset cone–rod dystrophy (CRD) with no visible macular degeneration.

Cases and methods: Case 1 was an 82-year-old man who first noticed a decrease in vision and color blindness in his early seventies. His mother and younger sister also had visual disturbances. His decimal visual acuity was 0.3 in the right eye and 0.2 in the left eye. Ophthalmoscopy showed normal fundi, and fluorescein angiography was also normal in both eyes. The photopic single flash and flicker eletroretinograms (ERGs) were severely attenuated and the scotopic ERGs were slightly reduced in both eyes. Case 2 was the 80-year-old younger sister of Case 1. She first noticed a decline in vision and photophobia in both eyes in her early seventies. Her decimal visual acuity was 0.4 in the right eye and 0.2 in the left eye. Ophthalmoscopy showed mottling of the retinal pigment epithelium in the midperiphery with no visible macular degeneration. The photopic single flash and flicker ERGs were severely attenuated, and the scotopic ERGs were slightly reduced in both eyes.

Conclusion: These siblings are the oldest reported cases of CRD with no visible macular degeneration. Thus, CRD should be considered in patients with reduced visual acuity, color blindness, and photophobia even if they are older than 70 years.

Keywords: cone–rod dystrophy, peripheral cone dystrophy, occult macular dystrophy, late onset, macular degeneration, negative ERG

Introduction

Cone–rod dystrophy (CRD) is an inherited retinal dystrophy that is characterized by reduced visual acuity, color blindness, and photophobia.[1–3] The age of onset generally ranges from the teens to the thirties,[2,3] and most patients with CRD have atrophic macular degeneration with a bull's eye lesion, or midperipheral degeneration in the late stages of the disease.[2,3] Patients with CRD can also have a central scotoma, and constriction of the peripheral visual fields at the end stages of the disease.[2,3] The cone-driven electroretinograms (ERGs) are attenuated even in the early stages, and this reduction is essential for making a diagnosis of CRD.[2,3]

Cases of atypical CRD, such as CRD with normal fundi,[4–7] occult macular dystrophy (OMD; Miyake disease),[8–11] peripheral cone dystrophy,[12–15] fundus albipunctatus associated with cone dystrophy,[16,17] and cone dystrophy with supernormal rod ERGs[18,19] have also been reported.

We present the clinical features of two siblings with CRD who had only mild fundus abnormalities. Their mother was also known to have visual difficulties, but was already dead at the time the two siblings were examined.

Correspondence: Kazuki Kuniyoshi
Department of Ophthalmology, Kinki University Faculty of Medicine, 377-2 Ohno-Higashi, Osaka-Sayama City, Osaka 589-8511, Japan
Tel +81 723 660 221
Fax +81 723 682 559
Email kazuki@med.kindai.ac.jp

Cases and methods

Our two cases were siblings who underwent ophthalmoscopy, visual acuity measurements, fundus fluorescein angiography (FA), Goldmann kinetic perimetry, Farnsworth D-15 test, Goldmann–Weekers dark adaptometry, full-field ERGs, multifocal ERGs (mfERGs), and optical coherence tomography (OCT). OCT images recorded from 24 age-matched normal subjects served as controls.

The ERGs and mfERGs were recorded according to the protocol recommended by the International Society for Clinical Electrophysiology of Vision. The mfERGs were recorded with the VERIS™ recording system (Electro-Diagnostic Imaging, Inc, Redwood, CA, USA). A Cirrus™ high-definition spectral-domain OCT instrument (Carl Zeiss Meditec AG, Jena, Germany) was used to obtain the OCT images.

Case reports

Case 1 was an 82-year-old man who first noticed a decrease in his vision and color vision in both eyes in his early seventies. His decimal best-corrected visual acuity (BCVA) at our initial examination was 0.3 oculus dexter (OD) with +3.25 diopters (D) and 0.2 oculus sinister (OS) with +3.25 D. His pupillary light reflexes and intraocular pressures were normal in both eyes. There was no history of the use of retinotoxic drugs. His cataracts were removed in both eyes at age 75; however, his vision was not improved.

Ophthalmoscopy showed that the fundus was normal in both eyes, and FA showed small hyperfluorescent spots at the parafoveal region of the left eye (Figure 1). Goldmann kinetic perimetry showed a central scotoma in both eyes (Figure 2), and Farnsworth D-15 test showed a tritan axis error. Goldmann–Weekers dark adaptometry revealed a slight elevation of the threshold in both eyes (Figure 3). The full-field scotopic ERGs elicited by both low- and high-intensity stimuli were slightly reduced. The scotopic b-wave elicited by a high-intensity stimulus was smaller than the a-wave, resulting in a negative-type ERG (Figure 4). On the other hand, photopic single-flash and 30 Hz flicker ERGs were severely attenuated in both eyes (Figure 4). The mfERGs were

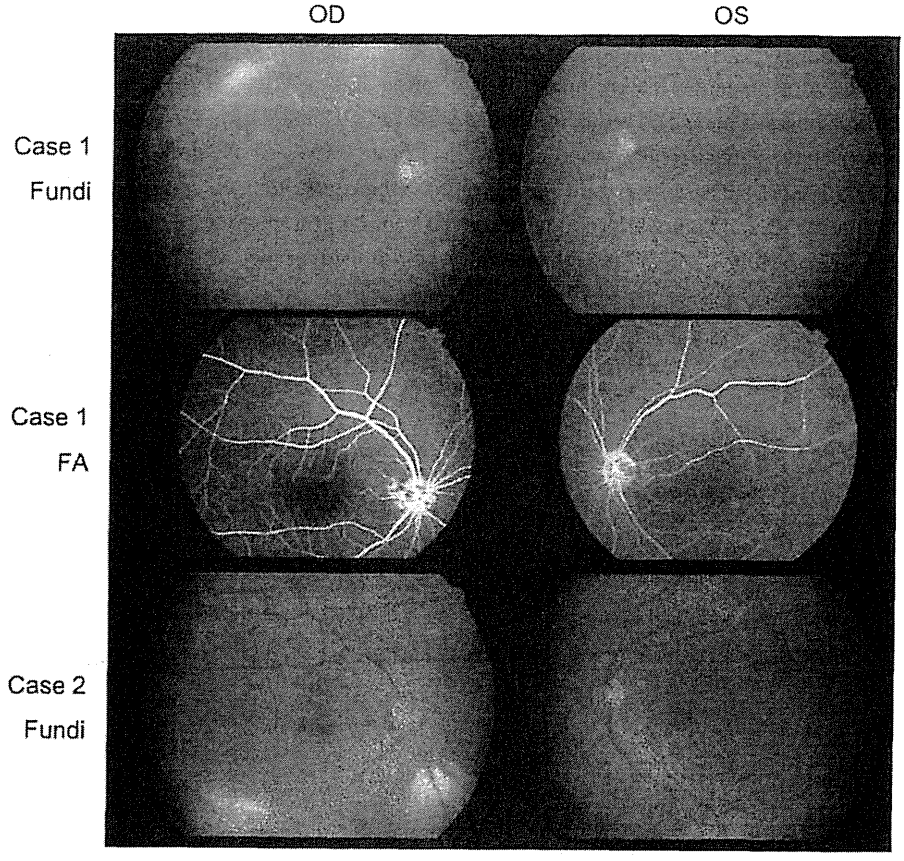

Figure 1 *Fundus photographs (Fundi) and FA.*
Abbreviations: OD, oculus dexter; OS, oculus sinister; FA, fluorescein fundus angiograms.

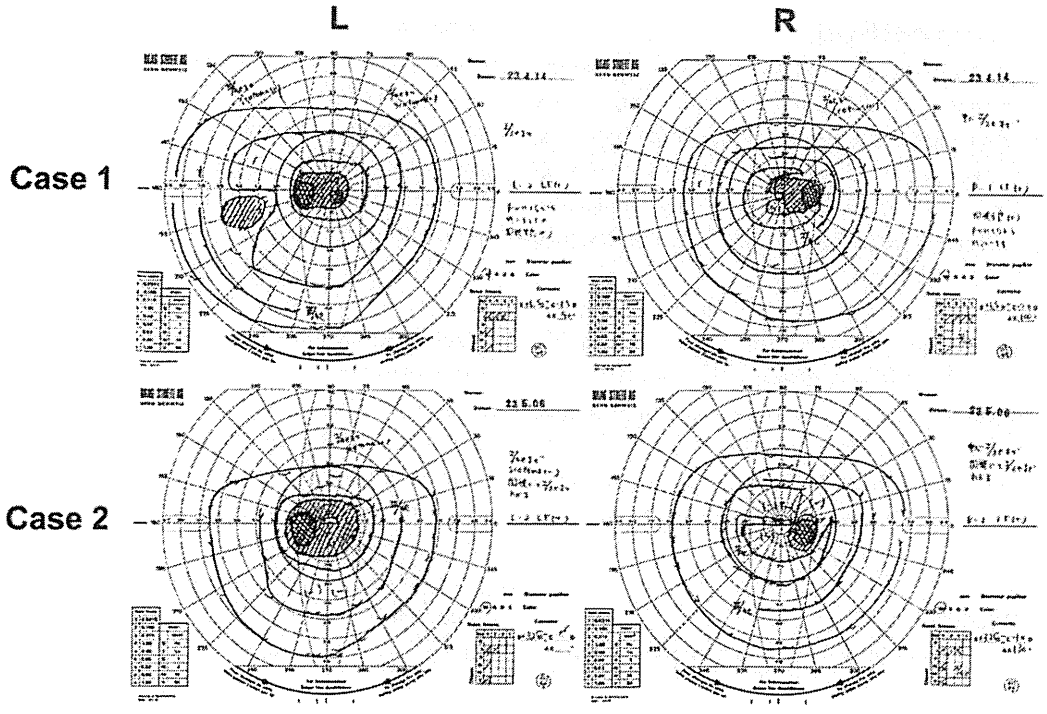

Figure 2 Results of Goldmann kinetic perimetry.
Abbreviations: L, left; R, right.

nonrecordable in the central area, but small responses were recorded in the midperiphery (Figure 5). The photoreceptor inner segment/outer segment junction line was indistinct in the OCT images (Figure 6). The thickness of the outer nuclear layer was 76 µm OD and 65 µm OS (normal mean 172 ± 17 µm) at the fovea, 65 µm OD and 43 µm OS (normal mean 128 ± 19 µm) at 0.5 mm superior to the fovea, and 65 µm OD and 54 µm OS (normal mean 135 ± 23 µm) at 0.5 mm inferior to the fovea. At 2 mm superior to the fovea, the thickness of the outer nuclear layer was 65 µm OD and 43 µm OS (normal mean 97 ± 13 µm), and at 2 mm inferior to the fovea it was 43 µm OD and 54 µm OS (normal

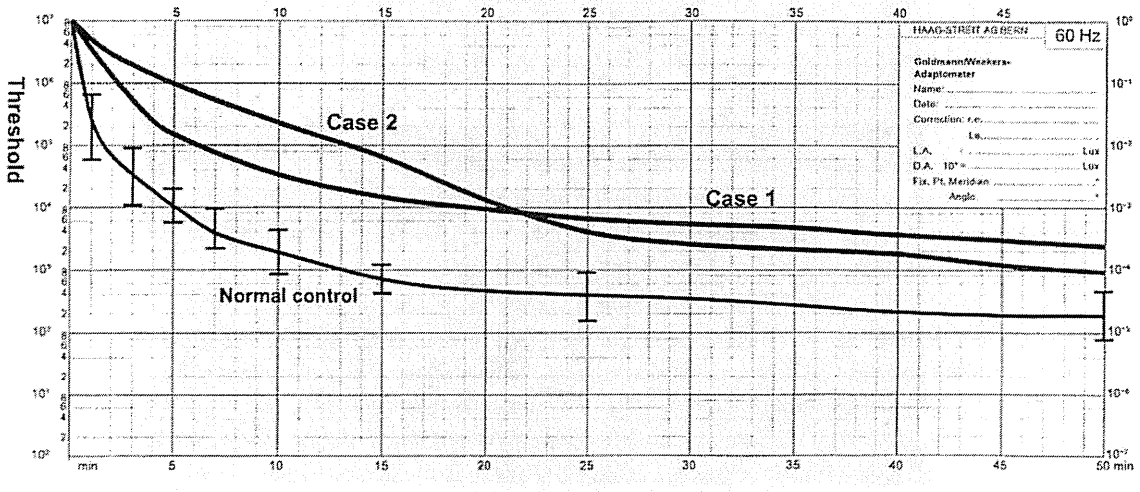

Figure 3 Results of Goldmann–Weekers dark adaptometry.
Note: The thin line indicates the average ± standard deviation isopter of normal controls.

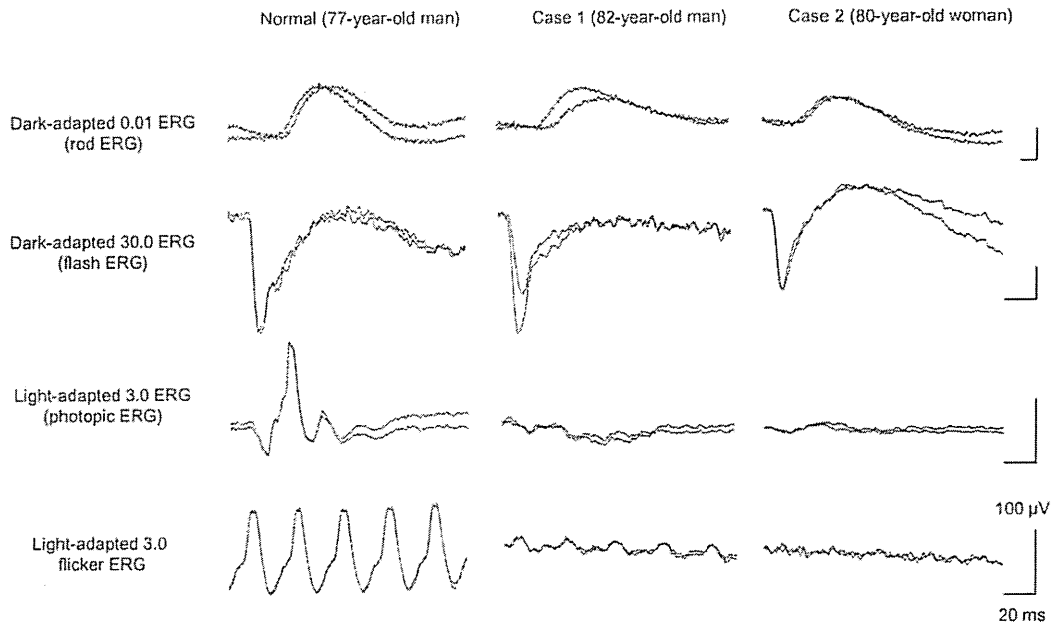

Figure 4 International Society for Clinical Electrophysiology of Vision-standard ERGs.
Note: The responses from both eyes are superimposed.
Abbreviation: ERG, electroretinography.

mean 88 ± 18 μm). Thus, the outer nuclear layer was thin, especially in the parafoveal region in both eyes (Figure 6). The thickness of the middle and inner layers of the retina were within normal limits.

Case 2 was the younger sister of case 1. She was 80 years old and had first noticed a decrease in her vision and photophobia in both eyes in her early seventies. Her cataract was removed in both eyes at age 76; however, her vision was not improved.

Our examination showed that her decimal BCVA was 0.4 OD with +0.25 D and 0.2 OS with +0.5 D. Her pupillary light reflexes and intraocular pressures were normal in both eyes. There was no history of retinotoxic drug use.

Her fundus was normal except for a slight mottling of the retinal pigment epithelium in the midperiphery. No macular degeneration was seen in either eye (Figure 1). FA was not performed because of her allergy to fluorescein sodium. Goldmann kinetic perimetry revealed a central scotoma in the left eye and a mild constriction of the visual fields in both eyes (Figure 2). Farnsworth D-15 test showed tritan axis errors in both eyes. Goldmann–Weekers dark adaptometry showed a slight elevation of the light threshold in both eyes (Figure 3). The full-field scotopic ERGs elicited by low-intensity stimuli were slightly reduced, and the scotopic high-intensity ERGs were normal, except the oscillatory potentials were reduced. The photopic single-flash and 30 Hz flicker ERGs were nonrecordable in both eyes (Figure 4). The mfERGs were nonrecordable in the right eye and reduced in the central and midperipheral areas of the left eye (Figure 5). OCT showed similar findings to her elder brother in the macular area (Figure 6). The photoreceptor inner segment/outer segment junction line was indistinct. The thickness of the outer nuclear layer was 130 μm OD and 129 μm OS (normal mean 172 ± 17 μm) at the fovea, 43 μm OD and 65 μm OS (normal mean 128 ± 19 μm) at 0.5 mm superior to the fovea, and 32 μm OD and 22 μm OS (normal mean 135 ± 23 μm) at 0.5 mm inferior to the fovea. At 2 mm superior to the fovea, the thickness of the outer nuclear layer was 65 μm OD and 76 μm OS (normal mean 97 ± 13 μm), and at 2 mm inferior to the fovea it was 65 μm OD and 43 μm OS (normal mean 88 ± 18 μm). Thus, the outer nuclear layer was thin, especially in the parafoveal region of both eyes (Figure 6).

Discussion

These two high-aged siblings, both in their eighties, had severely attenuated cone ERGs and mfERGs, and there was no evidence of visible macular abnormality. Case 1 had small hyperfluorescent spots in the fluorescein angiograms, and case 2 had mottling in the midperipheral fundus. Goldmann kinetic perimetry showed a central scotoma and reduced sensitivity in the area surrounding the scotoma in both patients. The mfERGs were nonrecordable in the foveal area, and only

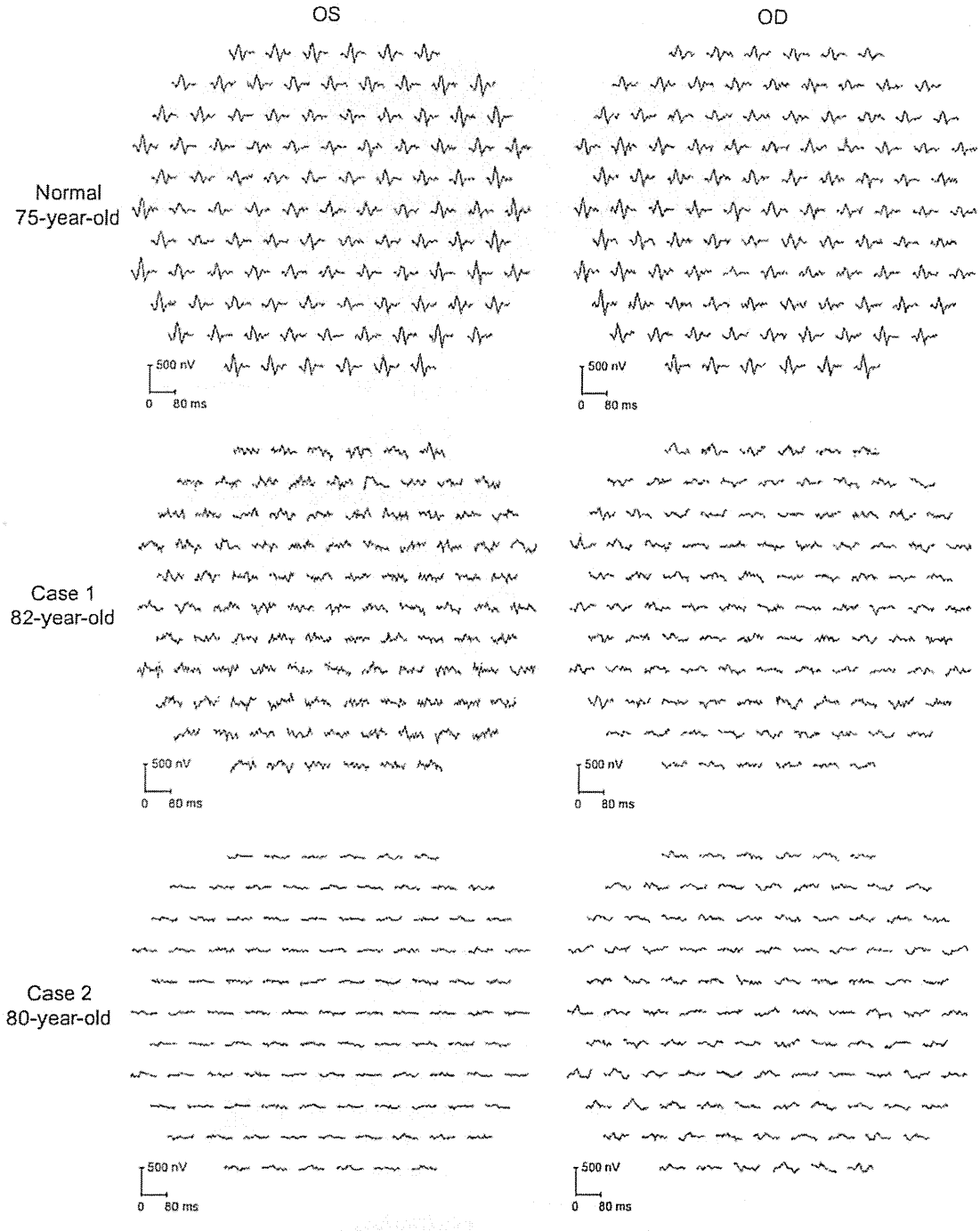

Figure 5 Multifocal ERGs.
Note: Responses were contaminated with much noise which was caused by photophobia.
Abbreviations: OS, oculus sinister; OD, oculus dexter; ERG, electroretinography.

very small responses were recorded in the midperiphery; these findings are consistent with results of the Goldmann kinetic perimetry.

We reviewed 497 CRD cases in 181 papers. Among these, 86 eyes in 43 patients in 20 papers were reported to have either normal fundus or only subtle fundus abnormalities (Figure 7).[4–7,20–35]

The vision of these cases is summarized in Figure 7, and the findings suggested that the vision in CRD cases with normal fundi is better than that in CRD cases with

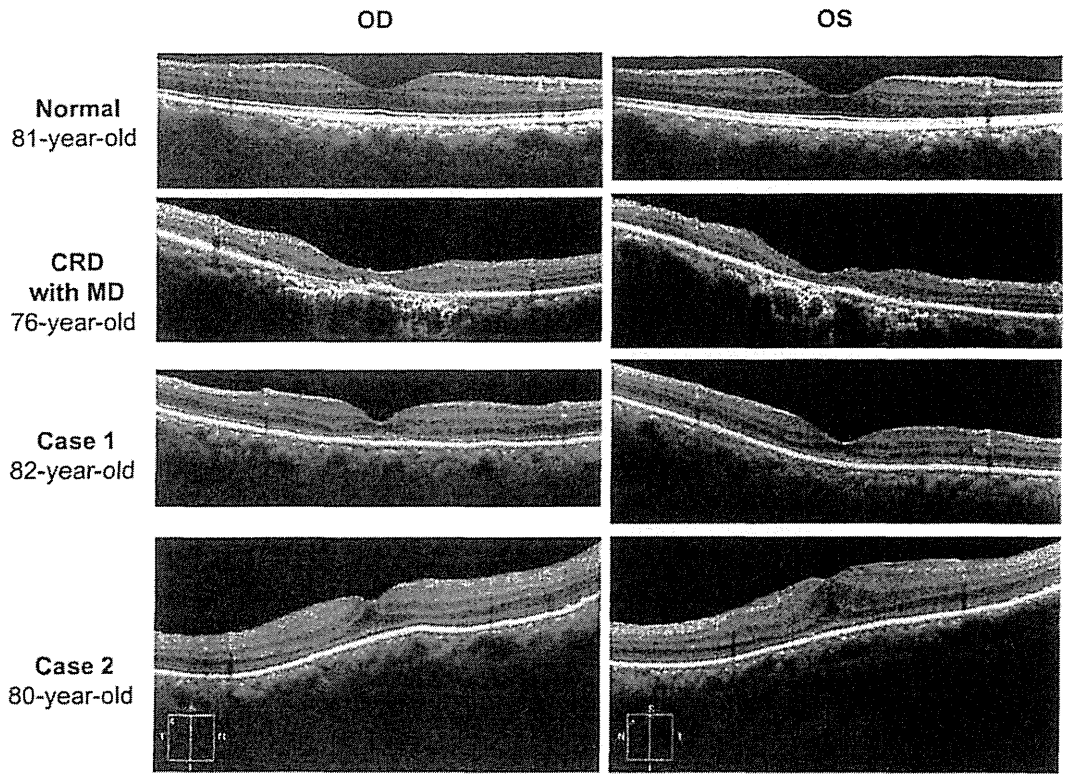

Figure 6 Results of optical coherence tomography.
Note: The photoreceptor inner segment/outer segment junction line is indistinct in the macular area.
Abbreviations: OD, oculus dexter; OS, oculus sinister; CRD, cone–rod dystrophy; MD, macular degeneration.

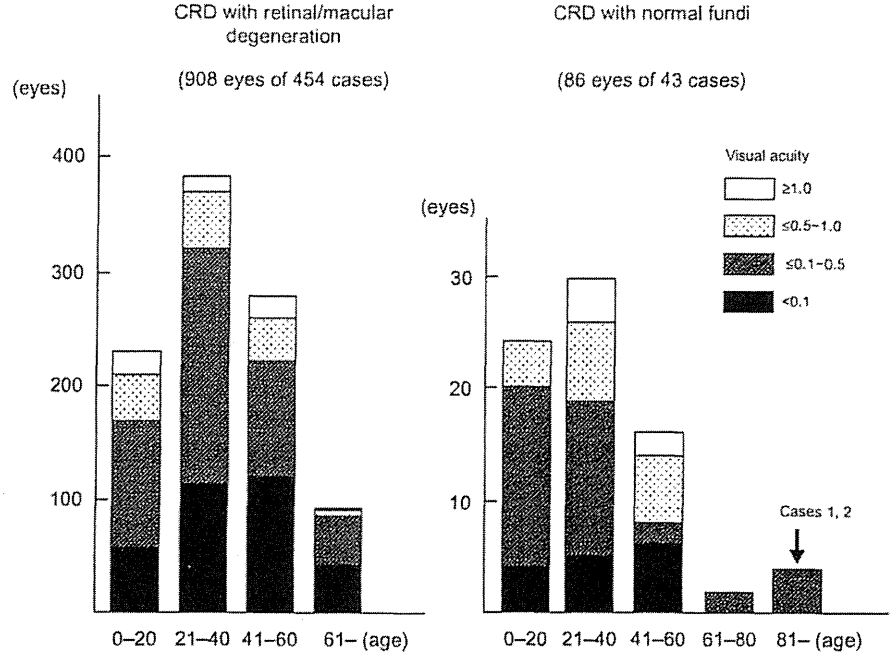

Figure 7 Age and visual acuity in cases with CRD in the past 181 papers published between 1963 and 2012.
Abbreviation: CRD, cone–rod dystrophy.

retinal/macular degeneration. Thirty-eight of 86 eyes (44%) with CRD and normal fundi had visual acuity better than 0.5, whereas 169 eyes of 908 eyes (19%) with retinal/macular degeneration had visual acuity better than 0.5.

Sixty-two of 86 eyes (72%) of the CRD cases with normal or subtle fundus abnormalities[4–7,20–35] had a family member with visible retinal degeneration, except the cases noted in studies by Ohba,[4] Rowe et al,[5] Miyake,[6] and Hayashi et al.[7] Ohba[4] reported on four CRD cases with normal fundi at ages 22 years, 23 years, 41 years, and 45 years. The patients' decimal BCVAs ranged from 0.1 to 0.07 in both eyes, and all were sporadic cases.[4] Rowe et al[5] reported four cases that were all sporadic and their ages were 55 years, 56 years, 60 years, and 68 years. Their decimal BCVAs ranged from 0.5 to 0.1 in both eyes.[5] Miyake[6] reported three cases of CRD with normal fundi from the same family whose ages were 32 years, 35 years, and 66 years. Their BCVAs were not reported. A sporadic, 53-year-old CRD case with normal fundi reported by Hayashi et al[7] had BCVAs of 0.1 OD and 0.7 OS.

CRD cases with normal fundi and no family history of retinal degeneration have a late onset, with an average age of 46 years and an average BCVA of 0.24. In comparison, the CRD cases with retinal or macular degeneration had an average age at onset of 23 years and the average BCVA was 0.09. The two siblings in our study had a very late onset with a positive family history and normal fundi. Their BCVAs after cataract removal ranged from 0.4 to 0.2 in both eyes, which are beyond the normal range reported,[36] and are comparable to the CRD cases with normal fundi and no family history of retinal degeneration.[4–7]

OMD is a kind of cone dystrophy with a normal fundus appearance.[8–11] Recently, a point mutation was found in the *RP1L1* gene in patients with autosomal-dominant OMD.[10] The ERG findings on our siblings are different from these cases of OMD because of the almost nonrecordable full-field cone response in our cases, which is due to diffuse cone dysfunction in these cases.

Peripheral cone dystrophy (or peripheral cone disease) is another kind of cone dystrophy that is characterized by cone dysfunction in the midperiphery to the periphery.[12–15] All of the past cases were reported as peripheral cone dystrophy and all had normal fundi. The gene mutation causing this cone dystrophy has not been identified. The results of mfERGs in our two cases were different from past cases of peripheral cone dystrophy because the mfERGs from the macula were nonrecordable. However, the two siblings in our study were probably at an advanced stage of the peripheral cone dystrophy because their outer nuclear layer at the fovea was well preserved compared with that of patients with cone dystrophy and a bull's eye lesion (Figure 6).

Several gene mutations have been identified in cases of CRD. Mutations of the *CRX* gene,[26,27,32,37–40] the *GUCY2D* gene,[29,33,35,41] the *GUCA1A* gene,[42] and *peripherin/RDS* gene[43] have been found in cases of autosomal-dominant CRD. Mutations of the *ABCA4* gene,[44] *CNGB3* gene,[28] and *KCNV2* gene,[19,30,31,34] have been reported for the autosomal-recessive cases of CRD. Mutations of the *CACNA1F* gene[45] and *RPGR* gene[46] have been detected in X-linked recessive cases of CRD.

Mutations of the *CRX* gene,[26,27,32] as well as the *GUCY2D*,[29,33,35] *KCNV2*,[30,31,34] and *CNGB3*[28] genes might be the cause of CRD in eyes with normal or mild fundus abnormalities. Cases with mutations in the *CRX* gene have diverse phenotypes ranging from Leber's congenital amaurosis[39,47] to CRD with normal fundi.[26,27,32] Sohocki et al[39] suggested that these varied phenotypes in patients with the *CRX*-gene mutations were due to deletion or point mutations in the gene. Deletion mutations in this gene would result in late-onset and mild CRD.[39] Our cases are similar to CRD cases with mutations in the *CRX* gene.

Swain et al[38] and Itabashi et al[40] reported CRD cases caused by a *CRX* gene mutation that had negative ERGs. Case 1 in our study had a reduced b-wave in the high-intensity ERGs that resembled the ERGs reported by Swain et al[38] and Itabashi et al.[40]

Mutations in other genes such as the *GUCY2D* gene,[26,27,32] *KCNV2* gene[30,31,34] and *CNGB3* gene[28] have also been reported to cause CRD with normal fundi; however, these patients were relatively young and some had supernormal rod responses, unlike our cases.

We investigated the gene in the siblings presented in our study using next-generation sequencing. However, detection of the causative mutation in these siblings was difficult because most of their family members, including their parents, were already deceased.

In summary, we report our findings in two siblings with late-onset CRD. Ophthalmoscopy showed that the macula was essentially normal in both cases. The scotopic ERGs were slightly reduced, but the photopic ERGs were nonrecordable. We recommended that older patients, >45 years of age, who had good vision earlier in their lives but had developed reduced vision, color vision abnormalities, and photophobia be examined by electroretinography to rule out CRD.

Acknowledgments

This research was supported in part by research grants from the Ministry of Health, Labor and Welfare, Japan, and Japan Society for the Promotion of Science, Japan.

Disclosure

The authors report no conflicts of interest in this work.

References

1. Steinmetz RD, Ogle KN, Rucker CW. Some physiologic considerations of hereditary macular degeneration. *Am J Ophthalmol*. 1956;42(4 Pt 2):304–319.
2. Krill AE, Deutman AF, Fishman M. The cone degenerations. *Doc Ophthalmol*. 1973;35(1):1–80.
3. Thiadens AA, Phan TM, Zekveld-Vroon RC, et al; Writing Committee for the Cone Disorders Study Group Consortium. Clinical course, genetic etiology, and visual outcome in cone and cone-rod dystrophy. *Ophthalmology*. 2012;119(4):819–826.
4. Ohba N. Progressive cone dystrophy; four cases of unusual form. *Jpn J Ophthalmol*. 1974;18(1):50–69.
5. Rowe SE, Trobe JD, Sieving PA. Idiopathic photoreceptor dysfunction causes unexplained visual acuity loss in later adulthood. *Ophthalmology*. 1990;97(12):1632–1637.
6. Miyake Y. Phenotypes of cone dysfunction syndrome. *Folia Ophthalmol Jpn*. 2000;51(8):725–733. Japanese.
7. Hayashi K, Yamada H, Wakakura M. A case of late-onset cone-rod dystrophy (CRD) which lacked ophthalmoscopic findings and diagnosed by electrophysiological examination. *Neuro-Ophthalmol Japan*. 2005;22(2):246–252. Japanese.
8. Miyake Y, Ichikawa K, Shiose Y, Kawase Y. Hereditary macular dystrophy without visible fundus abnormality. *Am J Ophthalmol*. 1989;108(3):292–299.
9. Miyake Y, Horiguchi M, Tomita N, et al. Occult macular dystrophy. *Am J Ophthalmol*. 1996;122(5):644–653.
10. Akahori M, Tsunoda K, Miyake Y, et al. Dominant mutations in *RP1L1* are responsible for occult macular dystrophy. *Am J Hum Genet*. 2010;87(3):424–429.
11. Tsunoda K, Usui T, Hatase T, et al. Clinical characteristics of occult macular dystrophy in family with mutation of *RP1L1* gene. *Retina*. 2012;32(6):1135–1147.
12. Pinckers A, Deutman AF. Peripheral cone disease. *Ophthalmologica*. 1977;174(3):145–150.
13. Kondo M, Miyake Y, Kondo N, Ueno S, Takakuwa H, Terasaki H. Peripheral cone dystrophy: a variant of cone dystrophy with predominant dysfunction in the peripheral cone system. *Ophthalmology*. 2004;111(4):732–739.
14. Okuno T, Oku H, Kurimoto T, Oono S, Ikeda T. Peripheral cone dystrophy in an elderly man. *Clin Experiment Ophthalmol*. 2008;36(9):897–899.
15. Baek J, Lee HK, Kim US. Spectral domain optical coherence tomography findings in bilateral peripheral cone dystrophy. *Doc Ophthalmol*. 2013;126(3):247–251.
16. Miyake Y, Shiroyama N, Sugita S, Horiguchi M, Yagasaki K. Fundus albipunctatus associated with cone dystrophy. *Br J Ophthalmol*. 1992;76(6):375–379.
17. Nakamura M, Hotta Y, Tanikawa A, Terasaki H, Miyake Y. A high association with cone dystrophy in Fundus albipunctatus caused by mutations of the *RDH5* gene. *Invest Ophthalmol Vis Sci*. 2000;41(12):3925–3932.
18. Gouras P, Eggers HM, MacKay CJ. Cone dystrophy, nyctalopia, and supernormal rod responses. A new retinal degeneration. *Arch Ophthalmol*. 1983;101(5):718–724.
19. Wu H, Cowing JA, Michaelides M, et al. Mutations in the gene *KCNV2* encoding a voltage-gated potassium channel subunit cause "cone dystrophy with supernormal rod electroretinogram" in humans. *Am J Hum Genet*. 2006;79(3):574–579.
20. Goodman G, Ripps H, Siegel IM. Cone dysfunction syndromes. *Arch Ophthalmol*. 1963;70:214–231.
21. Berson EL, Gouras P, Gunkel RD. Progressive cone degeneration, dominantly inherited. *Arch Ophthalmol*. 1968;80(1):77–83.
22. François J, de Rouck A, Verriest G, de Laey JJ, Cambie E. Progressive generalized cone dysfunction. *Ophthalmologica*. 1974;169(4):255–284.
23. Ripps H, Noble KG, Greenstein VC, Siegel IM, Carr RE. Progressive cone dystrophy. *Ophthalmology*. 1987;94(11):1401–1409.
24. van Schooneveld MJ, Went LN, Oosterhuis JA. Dominant cone dystrophy starting with blue cone involvement. *Br J Ophthalmol*. 1991;75(6):332–336.
25. Iijima H, Yamaguchi S, Kogure S, Hosaka O, Shibutani T. Electroretinogram in cone dystrophy. *Jpn J Ophthalmol*. 1991;35(4):453–466.
26. Jacobson SG, Cideciyan AV, Huang Y, et al. Retinal degenerations with truncation mutations in the cone-rod homeobox (*CRX*) gene. *Invest Ophthalmol Vis Sci*. 1998;39(12):2417–2426.
27. Tzekov RT, Sohocki MM, Daiger SP, Birch DG. Visual phenotype in patients with Arg41Gln and ala196+1 bp mutations in the *CRX* gene. *Ophthalmic Genet*. 2000;21(2):89–99.
28. Michaelides M, Aligianis IA, Ainsworth JR, et al. Progressive cone dystrophy associated with mutation in *CNGB3*. *Invest Ophthalmol Vis Sci*. 2004;45(6):1975–1982.
29. Smith M, Whittock N, Searle A, Croft M, Brewer C, Cole M. Phenotype of autosomal dominant cone-rod dystrophy due to the R838C mutation of the *GUCY2D* gene encoding retinal guanylate cyclase-1. *Eye (Lond)*. 2007;21(9):1220–1225.
30. Wissinger B, Dangel S, Jägle H, et al. Cone dystrophy with supernormal rod response is strictly associated with mutations in *KCNV2*. *Invest Ophthalmol Vis Sci*. 2008;49(2):751–757.
31. Ben Salah S, Kamei S, Sénéchal A, et al. Novel *KCNV2* mutations in cone dystrophy with supernormal rod electroretinogram. *Am J Ophthalmol*. 2008;145(6):1099–1106.
32. Kitiratschky VB, Nagy D, Zabel T, et al. Cone and cone-rod dystrophy segregating in the same pedigree due to the same novel *CRX* gene mutation. *Br J Ophthalmol*. 2008;92(8):1086–1091.
33. Kitiratschky VB, Wilke R, Renner AB, et al. Mutation analysis identifies *GUCY2D* as the major gene responsible for autosomal dominant progressive cone degeneration. *Invest Ophthalmol Vis Sci*. 2008;49(11):5015–5023.
34. Robson AG, Webster AR, Michaelides M, et al. "Cone dystrophy with supernormal rod electroretinogram": a comprehensive genotype/phenotype study including fundus autofluorescence and extensive electrophysiology. *Retina (Philadelphia, Pa)*. 2010;30(1):51–62.
35. Garcia-Hoyos M, Auz-Alexandre CL, Almoguera B, et al. Mutation analysis at codon 838 of the *guanylate cyclase 2D* gene in Spanish families with autosomal dominant cone, cone-rod, and macular dystrophies. *Mol Vis*. 2011;17:1103–1109.
36. Sjöstrand J, Laatikainen L, Hirvelä H, Popovic Z, Jonsson R. The decline in visual acuity in elderly people with healthy eyes or eyes with early age-related maculopathy in two Scandinavian population samples. *Acta Ophthalmol*. 2011;89(2):116–123.
37. Freund CL, Gregory-Evans CY, Furukawa T, et al. Cone-rod dystrophy due to mutations in a novel photoreceptor-specific homeobox gene (*CRX*) essential for maintenance of the photoreceptor. *Cell*. 1997;91(4):543–553.
38. Swain PK, Chen S, Wang QL, et al. Mutations in the cone-rod homeobox gene are associated with the cone-rod dystrophy photoreceptor degeneration. *Neuron*. 1997;19(6):1329–1336.
39. Sohocki MM, Sullivan LS, Mintz-Hittner HA, et al. A range of clinical phenotypes associated with mutations in *CRX*, a photoreceptor transcription-factor gene. *Am J Hum Genet*. 1998;63(5):1307–1315.

40. Itabashi T, Wada Y, Sato H, Kawamura M, Shiono T, Tamai M. Novel 615delC mutation in the CRX gene in a Japanese family with cone-rod dystrophy. *Am J Ophthalmol*. 2004;138(5):876–877.
41. Kelsell RE, Gregory-Evans K, Payne AM, et al. Mutations in the retinal guanylate cyclase (*RETGC-1*) gene in dominant cone-rod dystrophy. *Hum Mol Genet*. 1998;7(7):1179–1184.
42. Payne AM, Downes SM, Bessant DA, et al. A mutation in guanylate cyclase activator 1A (GUCA1A) in an autosomal dominant cone dystrophy pedigree mapping to a new locus on chromosome 6p21.1. *Hum Mol Genet*. 1998;7(2):273–277.
43. Nakazawa M, Kikawa E, Chida Y, Wada Y, Shiono T, Tamai M. Autosomal dominant cone-rod dystrophy associated with mutations in codon 244 (Asn244His) and codon 184 (Tyr184Ser) of the peripherin/RDS gene. *Arch Ophthalmol*. 1996;114(1):72–78.
44. Cremers FP, van de Pol DJ, van Driel M, et al. Autosomal recessive retinitis pigmentosa and cone-rod dystrophy caused by splice site mutations in the Stargardt's disease gene *ABCR*. *Hum Mol Genet*. 1998;7(3):355–362.
45. Jalkanen R, Mäntyjärvi M, Tobias R, et al. X linked cone-rod dystrophy, CORDX3, is caused by a mutation in the *CACNA1F* gene. *J Med Genet*. 2006;43(8):699–704.
46. Demirci FY, Rigatti BW, Wen G, et al. X-linked cone-rod dystrophy (locus *COD1*): identification of mutations in *RPGR* exon ORF15. *Am J Hum Genet*. 2002;70(4):1049–1053.
47. Freund CL, Wang QL, Chen S, et al. De novo mutations in the *CRX* homeobox gene associated with Leber congenital amaurosis. *Nat Genet*. 1998;18(4):311–312.

Hindawi Publishing Corporation
BioMed Research International
Volume 2013, Article ID 676803, 12 pages
http://dx.doi.org/10.1155/2013/676803

Hindawi

Clinical Study

High-Resolution *En Face* Images of Microcystic Macular Edema in Patients with Autosomal Dominant Optic Atrophy

Kiyoko Gocho,[1] Sachiko Kikuchi,[1] Takenori Kabuto,[1] Shuhei Kameya,[1] Kei Shinoda,[2] Atsushi Mizota,[2] Kunihiko Yamaki,[1] and Hiroshi Takahashi[3]

[1] *Department of Ophthalmology, Nippon Medical School Chiba Hokusoh Hospital, 1715 Kamagari, Inzai, Chiba 270-1694, Japan*
[2] *Department of Ophthalmology, Teikyo University School of Medicine, 2-11-1 Kaga, Itabashi-ku, Tokyo 173-8605, Japan*
[3] *Department of Ophthalmology, Nippon Medical School, 1-1-5 Sendagi, Bunkyo-ku, Tokyo 113-8602, Japan*

Correspondence should be addressed to Shuhei Kameya; shuheik@nms.ac.jp

Received 7 August 2013; Revised 21 October 2013; Accepted 4 November 2013

Academic Editor: Marcela Votruba

The purpose of this study was to investigate the characteristics of microcystic macular edema (MME) determined from the *en face* images obtained by an adaptive optics (AO) fundus camera in patients with autosomal dominant optic atrophy (ADOA) and to try to determine the mechanisms underlying the degeneration of the inner retinal cells and RNFL by using the advantage of AO. Six patients from 4 families with ADOA underwent detailed ophthalmic examinations including spectral domain optical coherence tomography (SD-OCT). Mutational screening of all coding and flanking intron sequences of the *OPA1* gene was performed by DNA sequencing. SD-OCT showed a severe reduction in the retinal nerve fiber layer (RNFL) thickness in all patients. A new splicing defect and two new frameshift mutations with premature termination of the Opa1 protein were identified in three families. A reported nonsense mutation was identified in one family. SD-OCT of one patient showed MME in the inner nuclear layer (INL) of the retina. AO images showed microcysts in the *en face* images of the INL. Our data indicate that AO is a useful method to identify MME in neurodegenerative diseases and may also help determine the mechanisms underlying the degeneration of the inner retinal cells and RNFL.

1. Introduction

Autosomal dominant optic atrophy (ADOA; MIM no. 165500), also known as Kjer's disease [1], is the most common hereditary ocular neuropathy with a prevalence of 1/12,000–1/50,000 [2–4]. ADOA is characterized by a decrease in the visual acuity that develops in childhood, temporal palor of the optic discs, centrocecal scotoma, and color vision defects [5, 6]. Histopathological studies of human eyes with ADOA showed diffuse atrophy of the retinal ganglion cell (RGC) layer that predominated in the central retina [7, 8].

ADOA has considerable intra- and interfamilial clinical variability with incomplete penetrance estimated to be about 90% in the familial forms of the disease [9]. Mutations in the optic atrophy 1 gene, *OPA1* (MIM no. 605290), located on chromosome 3q28-q29, are responsible for about 60–80% of the cases of ADOA [10–12].

OPA1 encodes a mitochondrial dynamin-related GTPase, which is anchored to the mitochondrial inner membrane [13, 14]. Although the Opa1 protein is ubiquitously expressed in human tissues, a strong expression of the Opa1 protein has been reported in the RGC layer [15]. The Opa1 protein has multiple functions and plays a key role in the fusion of mitochondria and thus in organizing the mitochondrial network [13, 14]. The other functions of the Opa1 protein are related to oxidative phosphorylation, maintenance of the membrane potential [11, 16, 17], maintenance of mtDNA [18, 19], organizing the cristae, and control of mitochondrial apoptosis through the compartmentalization of cytochrome C [17, 20]. Mutations of the *OPA1* gene result in a loss of function in most ADOA patients indicating that haploinsufficiency is involved in the pathomechanism of the disease [21]. However, to date, there is no clear evidence to suggest a further role for the *OPA1* gene in the degeneration of RGCs in ADOA.

Recently, Barboni et al. detected "microcystic macular edema (MME)" in the inner nuclear layer (INL) of